Succinyl-CoA-based energy metabolism dysfunctions in chronic heart failure

Shingo Takada (s-takada@hotmail.co.jp)
Hokkaido University Graduate School of Medicine https://orcid.org/0000-0002-7781-9482

Satoshi Maekawa
Department of Cardiovascular Medicine, Faculty of Medicine and Graduate School of Medicine, Hokkaido University

Takaaki Furihata
Department of Cardiovascular Medicine, Faculty of Medicine and Graduate School of Medicine, Hokkaido University

Naoya Kakutani
Department of Cardiovascular Medicine, Faculty of Medicine and Graduate School of Medicine, Hokkaido University

Daiki Setoyama
Department of Clinical Chemistry and Laboratory Medicine, Graduate School of Medical Sciences, Kyushu University

Koji Ueda
Japanese Foundation For Cancer Research https://orcid.org/0000-0001-9066-4959

Hideo Nambu
Department of Cardiovascular Medicine, Faculty of Medicine and Graduate School of Medicine, Hokkaido University

Hikaru Hagiwara
Department of Cardiovascular Medicine, Faculty of Medicine and Graduate School of Medicine, Hokkaido University

Haruka Handa
Hokkaido University https://orcid.org/0000-0002-8557-7479

Yoshizuki Fumoto
Department of Molecular Biology, Faculty of Medicine and Graduate School of Medicine, Hokkaido University

Soichiro Hata
Department of Molecular Biology, Faculty of Medicine and Graduate School of Medicine, Hokkaido University

Arata Fukushima
Hokkaido University Graduate School of Medicine

Takashi Yokota

Hokkaido University Graduate School of Medicine https://orcid.org/0000-0001-5470-6648

Dongchon Kang

Graduate School of Medical Sciences, Kyushu University

Shintaro Kinugawa

Department of Cardiovascular Medicine, Faculty of Medicine and Graduate School of Medicine, Hokkaido University

Hisataka Sabe

Hokkaido University Graduate School of Medicine

Article

Keywords:

Posted Date: December 7th, 2021

DOI: https://doi.org/10.21203/rs.3.rs-838227/v1

Succinyl-CoA-based energy metabolism dysfunctions in chronic heart failure (74 < 75 characters/spaces)

Shingo Takada[1,2,3,†*]✉, Satoshi Maekawa[1†], Takaaki Furihata[1], Naoya Kakutani[1], Daiki Setoyama[4], Koji Ueda[5], Hideo Nambu[1], Hikaru Hagiwara[1], Haruka Handa[2], Yoshizuki Fumoto[2], Soichiro Hata[2], Arata Fukushima[1], Takashi Yokota[1], Dongchon Kang[4,6], Shintaro Kinugawa[1,7*]✉, and Hisataka Sabe[2*]✉

[1]Department of Cardiovascular Medicine, [2]Department of Molecular Biology, Hokkaido University Graduate School of Medicine, Sapporo, Japan; [3]Department of Lifelong Sport, School of Sports Education, Hokusho University, Ebetsu, Japan; [4]Department of Clinical Chemistry and Laboratory Medicine; [5]Cancer Precision Medicine Center, Japanese Foundation for Cancer Research, Tokyo, Japan; [6]Clinical Laboratories, Kyushu University Hospital, Fukuoka, Japan; [7]Department of Cardiovascular Medicine, Graduate School of Medical Sciences, Kyushu University, Fukuoka, Japan

[†] These authors contributed equally to this work.

✉e-mail:

*s-takada@hokusho-u.ac.jp (S.T.);

*kinugawa@cardiol.med.kyushu-u.ac.jp (S.K.);

*sabeh@med.hokudai.ac.jp (H.S.)

(Abstract)

Heart failure (HF) is a leading cause of death and repeated hospitalizations[1]. HF progression generally involves mitochondrial dysfunction[2-4]. However, how mitochondria react to chronic HF remains unclear. Here, we show the molecular basis of mitochondrial dysfunction in chronic HF, which is characterized by altered succinyl-CoA metabolism. In myocardial mitochondria of coronary ligated mice, heme synthesis and ketolysis, and enzymes using succinyl-CoA in these events were upregulated, and enzymes synthesizing succinyl-CoA at the tricarboxylic acid (TCA) cycle were also increased. Intriguingly, the ADP-specific, but not the GDP-specific, subunit of succinyl-CoA synthetase, which uses succinyl-CoA in the TCA cycle, was decreased. Myocardial succinyl-CoA levels were significantly reduced in chronic HF, impairing mitochondrial oxidative phosphorylation (OXPHOS). Consequently, the administration of 5-aminolevulinic acid (ALA)[5], an intermediate in the pathway from succinyl-CoA to heme synthesis, prevented HF progression in mice. Previous reports also support the presence of succinyl-CoA metabolism abnormalities in HF patients[6,7]. Our results indicated that changes in succinyl-CoA usage in various energy production systems in myocardial mitochondria is characteristic to chronic HF, and that although similar alterations occur in healthy conditions, such as during strenuous exercise, they may often occur irreversibly in HF. Moreover, nutritional interventions compensating the metabolic changes are likely to provide effective methods to treat HF. (207 < approx. 200 words)

(text)

Mitochondrial dysfunction is frequently involved in the development of HF, and metabolic dysfunction, including that of the TCA cycle, a core metabolic pathway for producing ATP, is known as the main cause[2-4]. Recent studies have shown that the selective accumulation of succinate, an intermediate of the TCA cycle, during acute ischemia in the mouse heart is a major cause of reperfusion injury[8-10]. On the other hand, how the TCA cycle and its associated energy-producing metabolic pathways respond to chronic HF remains largely unclear. We here addressed this question with the aim of understanding the metabolic basis of mitochondrial dysfunction in chronic HF. We used a mouse model of HF, in which myocardial infarction (MI) was induced by permanent left anterior descending coronary artery ligation[11,12]. Mice with permanent coronary artery ligation (hereafter referred to as MI mice) generally start to show HF symptoms 7 days after the ligation[11,12], which we also confirmed in this study (Extended Data Fig. 1). Sham-operated mice were used as a control[11,12]. We used these mice 28 days after surgery in all the following analyses, unless otherwise described, and excluded necrotic areas of MI mice from biochemical analyses.

Extended data Fig. 1

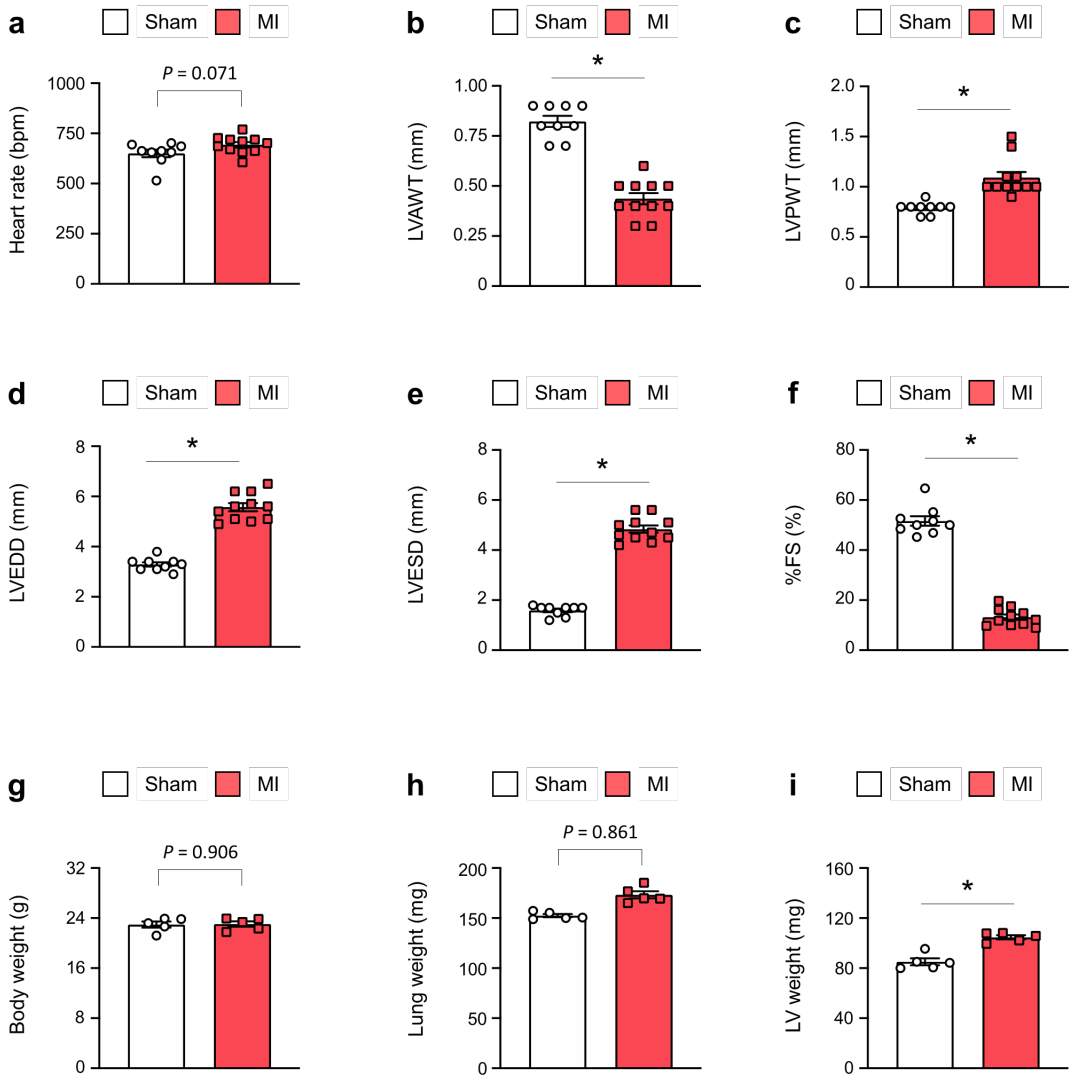

Extended Data Figure 1. Cardiac parameters of the MI mice and sham mice used in this study. MI mice and sham mice used in our experiments were randomly sampled, and their cardiac parameters, namely heart rate (**a**), LV anterior wall thickness (LVAWT) (**b**), LV posterior wall thickness (LVPWT) (**c**), LV end-diastolic diameter (LVEDD) (**d**), LV end-systolic diameter (ESD) (**e**), %FS (**f**), body weight (**g**), lung weight (**h**), and LV weight (**i**).

Succinyl-CoA decreases in chronic HF (37/40 characters)

To investigate the possible metabolic changes in the mouse heart during chronic HF, we first analyzed the levels of TCA cycle intermediates. Liquid chromatography-mass spectrometry (LC-MS)-based analysis demonstrated a significant selective reduction in succinyl-CoA level in cardiac muscles of MI mice compared with those of sham mice (Fig. 1). The majority of succinyl-CoA is produced by the TCA cycle[13]. Levels of other TCA cycle intermediates, including succinate, did not show a statistically significant difference between MI mice and sham mice (Fig. 1). Therefore, it is likely that metabolic changes occur in the myocardial muscle of mice during chronic HF that are very different from those that occur during acute ischemia[8].

Fig. 1

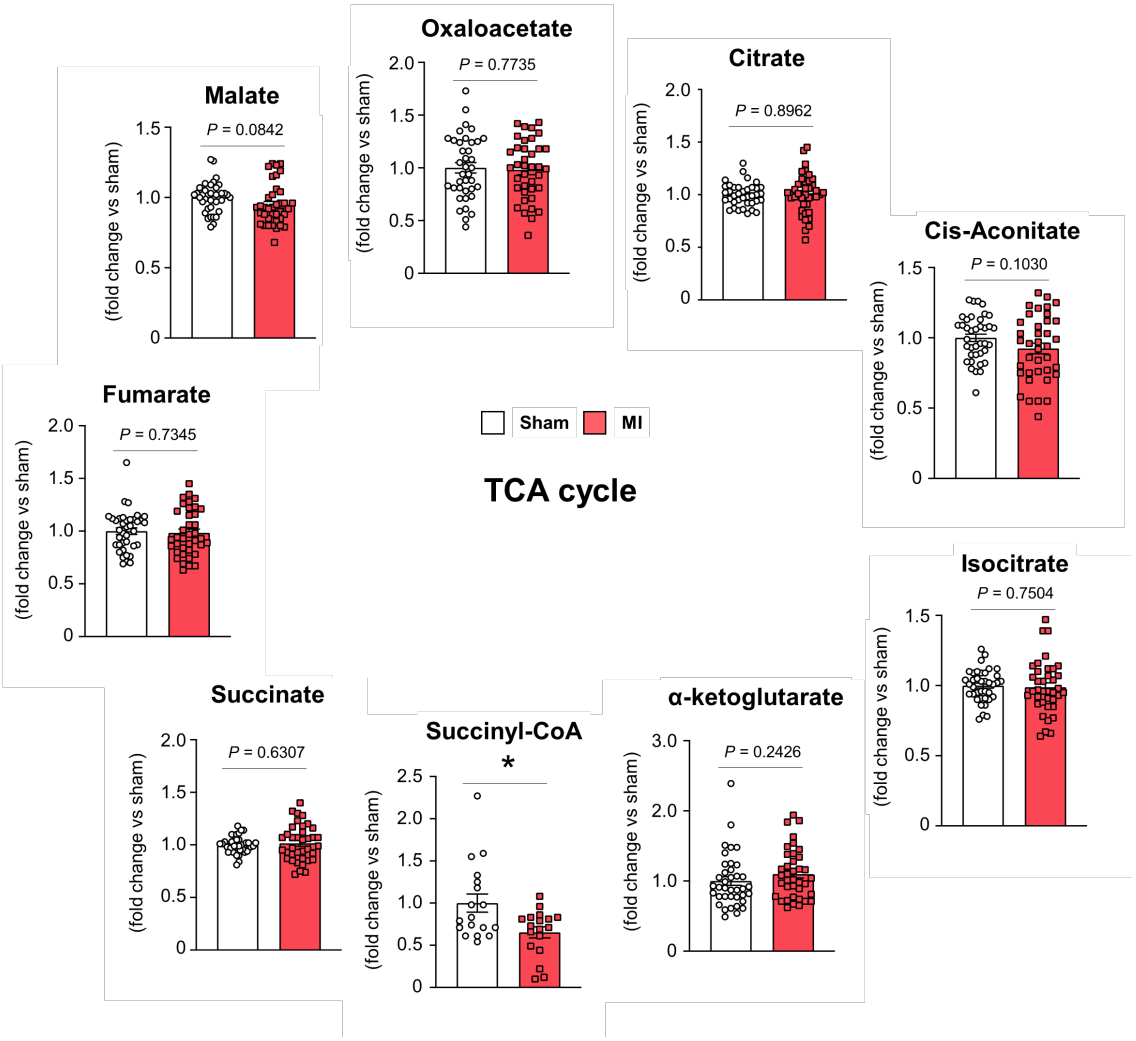

Fig. 1. Selective reduction of succinyl-CoA among the TCA cycle metabolites in cardiac muscle during chronic HF. Relative levels of the TCA cycle metabolites in cardiac muscles isolated from MI mice, compared with those from sham mice, 28 days after surgery. Each data point in the dot plot represents one individual mouse sample (n = 38 for both groups for all metabolites, except for succinyl-CoA in which n = 18 for both groups). Data are shown as the mean ± s.e.m. The two-tailed Student t-test was performed for pairwise comparisons. *$P < 0.05$.

Enzyme levels change in chronic HF (34/40 characters)

We then sought to understand the molecular bases of this reduction in succinyl-CoA level. For this purpose, we investigated the expression levels of enzymes associated with succinyl-CoA metabolism, by analyzing mitochondria isolated from cardiac muscle. The E1 component of the 2-oxoglutarate dehydrogenase (Ogdh) complex, which generates succinyl-CoA from alpha-ketoglutarate (αKG) in the TCA cycle (see Fig. 2a), was significantly increased in MI mice compared with sham mice (Fig. 2b). MI mice also showed increased levels of glutamate dehydrogenase 1 (Glud1), which catalyzes the reversible reaction of glutamate to αKG (Fig. 2c). On the other hand, changes in the levels of propionyl-CoA carboxylase α (Pcca) and methylmalonyl-CoA mutase (Mcm), which are involved in the synthesis of succinyl-CoA from fatty acids and several amino acids, did not show a clear statistical difference between MI mice and sham mice (Fig. 2 d, e, f). Succinyl-CoA synthetase catalyzes the reversible reaction of succinyl-CoA to succinate in the TCA cycle (see Fig. 1a). The noncatalytic ADP-specific β subunit (Sucla2) and the catalytic α subunit (Suclg1) of this enzyme were significantly decreased in MI mice compared with sham mice, although the extent of the decrease in Sucla2 was more prominent (Fig. 2g). On the other hand, expression of the noncatalytic GDP-specific β subunit (Suclg2) did not change significantly (Fig. 2g). However, these changes appeared to be favorable for the synthesis of succinyl-CoA from its precursors and for the downregulation of the incorporation of succinyl-CoA into the TCA cycle, and hence could not explain the selective reduction of succinyl-CoA that we above observed.

There are several other pathways that utilize succinyl-CoA in the mitochondrion,

113 namely, heme synthesis and ketolysis[13]. Heme is essential for mitochondrial OXPHOS.
114 Mitochondrial heme synthesis is initiated from the synthesis of ALA, which is
115 synthesized from succinyl-CoA and glycine by the mitochondrial rate-limiting enzyme
116 5′-aminolevulinate synthase 1 (Alas1) (ref.[5,14]) (see Fig. 2h). In the myocardial
117 mitochondria of MI mice, levels of Alas1 and heme were significantly increased
118 compared with sham mice (Fig. 2i, j). On the other hand, it is well documented that the
119 utilization of ketone bodies as an energy source is upregulated in the heart in proportion
120 to the level of plasma ketone bodies, accompanied by the increased production of ketone
121 bodies in the liver, in both HF patients and animal models[15,16]. In mitochondrial ketolysis,
122 ketone bodies are converted into acetyl-CoA (see Fig. 2k). Consistently, β-
123 hydroxybutyric acid (β-OHB), a major component of ketone bodies, was significantly
124 increased in the plasma but was significantly reduced in the cardiac muscles of MI mice
125 compared with sham mice (Fig. 2l, m). Moreover, the level of 3-oxoacid CoA-transferase
126 1 (Oxct1), which is the main catalyst of ketone bodies via the use of succinyl-CoA (see
127 Fig. 2k), was significantly upregulated in the myocardial mitochondria of MI mice (Fig.
128 2n). Therefore, collectively, our results suggest that the myocardial mitochondria of mice
129 undergo metabolic changes during chronic HF, in which levels of enzymes that utilize
130 succinyl-CoA for heme synthesis and ketolysis are increased, and the level of an enzyme
131 that utilizes succinyl-CoA in the TCA cycle is decreased. Moreover, although these
132 changes also involve increased levels of enzymes that synthesize succinyl-CoA from αKG
133 and glutamate, our results suggested that these changes often result in reduced succinyl-
134 CoA levels. Binding sites of hypoxia-inducible factor 1 are found in the *ALAS1/Alas1*
135 promoter regions in both humans and mice (http://jaspar.genereg.net/), although *ALAS1*
136 mRNA is not always upregulated under hypoxia[17]. Increased heme levels in the failing

hearts of mice have also been reported previously, but the upregulation of Alas1 has not been shown to date[18]. Downregulation of the forward reaction of the TCA cycle may suppress production of reactive oxygen species in mitochondria under lowered oxygen concentrations[8]. Moreover, not only failing hearts, but some other organs, including skeletal muscle under healthy conditions also utilize ketone bodies, such as during long-lasting vigorous physical exercise[19], although whether levels of the enzymes involved also change in healthy conditions is unknown. Thus, taken together, myocardial mitochondria in chronic HF may undergo a hitherto unknown mode of metabolic dysfunction, although many of the events involved in this dysfunction are known physiological responses of mitochondria. It should be noted, however, that many issues remain unsolved, including the molecular basis of the altered enzyme levels in chronic HF, as well as whether these metabolic shifts are associated with cardiac remodeling during chronic HF.

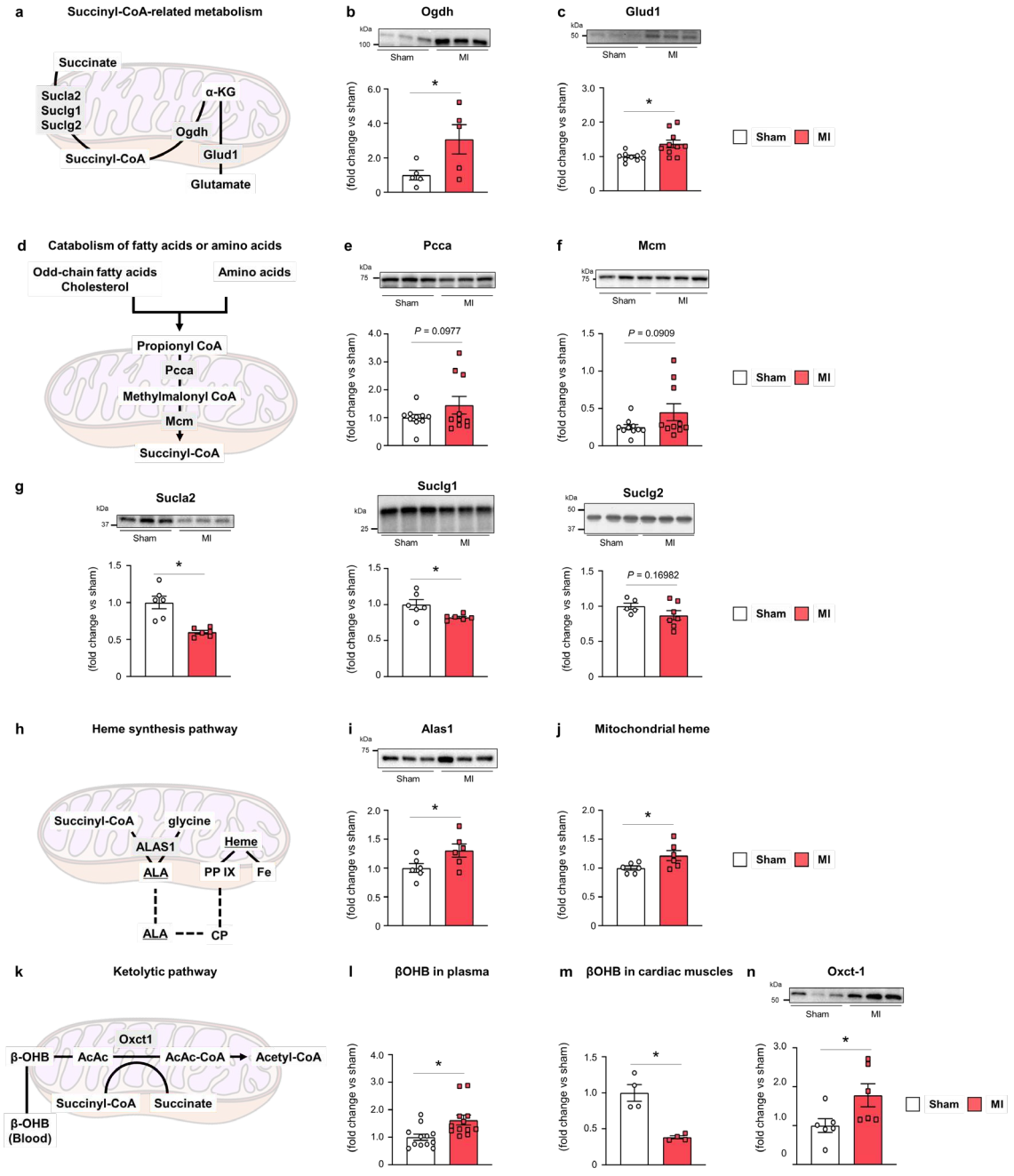

Fig. 2. Enzyme level changes in myocardial mitochondria during chronic HF promote heme synthesis and ketolysis, and downregulate the incorporation of succinyl-CoA into the TCA cycle. a-c, Succinyl-CoA metabolism in the TCA cycle (**a**); and relative protein levels of Ogdh (**b**) (n = 5) and Glud1 (**c**) (n = 10). **d-f**, Propionyl-CoA-based succinyl-CoA synthesis in the mitochondrion (**a**); and relative protein levels

of Pcca (**e**) (n = 10) and Mcm (**f**) (n = 10). **g**, Relative protein levels of the succinyl-CoA synthetase subunits Sucla2 (*left*, n = 6), Suclg1 (*middle*, n = 6) and Suclg2 (*right*, n = 6). **h**-**j**, Heme synthesis pathway in the mitochondrion (**h**); and relative protein levels of Alas1 (**i**) (n = 6) and relative amounts of heme (**j**) (n = 6). CP, coproporphyrinogen-III; and PPIX, protoporphyrin IX. **k-n,** Ketolytic pathway in the mitochondrion (**k**); and relative amounts of β-OHB in plasma (**l**) (n = 12) and cardiac muscle (**m**) (n = 4), and relative levels of Oxct1 in mitochondria (**n**) (n = 6). All assays were performed using isolated myocardial mitochondria, except for **l** (blood plasma) and **m** (cardiac muscle). In **b**, **c**, **e**, **f**, **g**, **i**, and **n**, representative results of each immunoblot blot are shown in the upper panels. Each data point in the dot plot represents one individual mouse sample. Data are shown as the mean ± s.e.m. The two-tailed Student t-test was performed for pairwise comparisons. *$P < 0.05$. Full-size CBB staining scans of the immunoblots are shown in Extended Data Fig. 5.

Succinyl-CoA reduction impairs OXPHOS (38/40 characters)

We then addressed whether a decreased succinyl-CoA level impairs mitochondrial OXPHOS capacity. We previously showed that both complex I (CI)-linked (*i.e.*, NADH-driven CI/complex III [CIII]/complex IV [CIV] supercomplex) and complex II (CII)-linked (*i.e.*, FADH-driven CII/CIII/CIV chain) OXPHOS capacities are decreased in the myocardial mitochondria of MI mice[20], which we hereby confirmed again (Fig. 3a). The addition of 1 mM succinyl-CoA to isolated myocardial mitochondria of MI mice increased their CI- and CII-linked OXPHOS capacities to levels almost comparable to those of sham mice (Fig. 3a). Myocardial mitochondria isolated from non-operated mice

did not show this positive response to succinyl-CoA (Fig. 3b), and even 3 mM and 10 mM succinyl-CoA still did not increase OXPHOS activity, but rather impaired it (Fig. 3b). On the other hand, 1 to 10 mM succinate did not show such effects (Fig. 3c). Therefore, these results indicate that the decrease in succinyl-CoA level in the cardiac muscle of mice during chronic HF is likely to contribute to the reduced CI- and CII-linked OXPHOS capacities of the failing heart. CI requires NADH for its activity, and CII is driven by succinate dehydrogenase (Sdh)[2,21]. Thus, our results imply that the decreased level of succinyl-CoA affects some reactions of the TCA cycle that produce NADH, and also downregulates the forward reaction of Sdh. Impaired CII activity, as well as the increased level of Oxct1, which generates succinate from succinyl-CoA, of the myocardial mitochondria of MI mice would explain, at least in part, why the level of succinate was not notably changed, despite the reduced succinyl-CoA level. On the other hand, our results posed the simple question as to why the external addition of succinyl-CoA did not upregulate the OXPHOS capacity of intact mitochondria, although it upregulated this capacity in the myocardial mitochondria of MI mice.

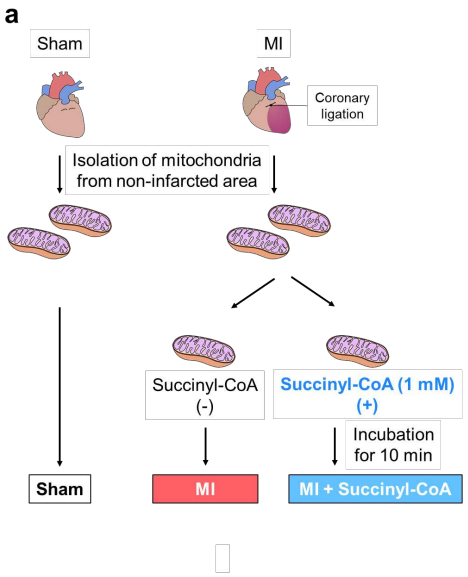
a
Sham
MI
Coronary ligation
Isolation of mitochondria from non-infarcted area
Succinyl-CoA (-)
Succinyl-CoA (1 mM) (+)
Incubation for 10 min
Sham
MI
MI + Succinyl-CoA

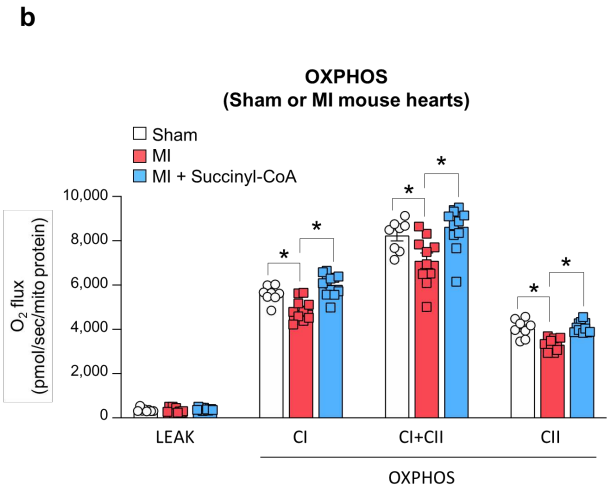
b
OXPHOS
(Sham or MI mouse hearts)
Sham
MI
MI + Succinyl-CoA
O2 flux (pmol/sec/mito protein)
10,000
8,000
6,000
4,000
2,000
0
LEAK
CI
CI+CII
CII
OXPHOS

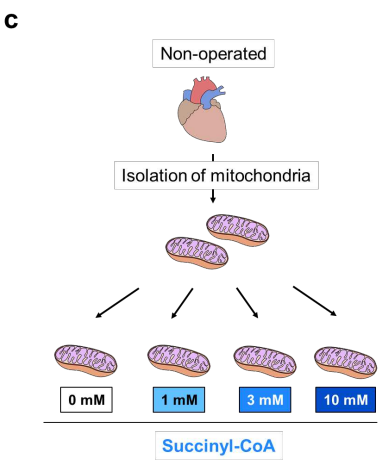
c
Non-operated
Isolation of mitochondria
0 mM
1 mM
3 mM
10 mM
Succinyl-CoA

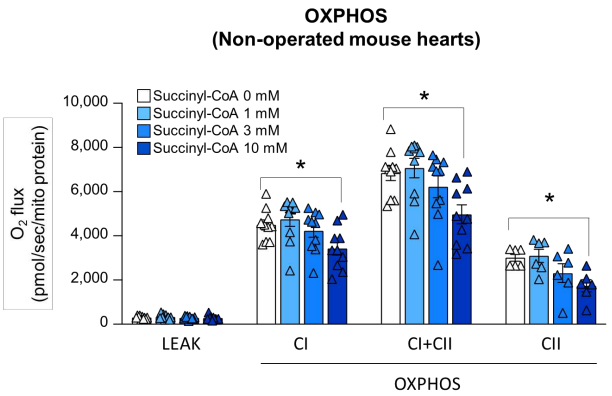
d
OXPHOS
(Non-operated mouse hearts)
Succinyl-CoA 0 mM
Succinyl-CoA 1 mM
Succinyl-CoA 3 mM
Succinyl-CoA 10 mM
O2 flux (pmol/sec/mito protein)
10,000
8,000
6,000
4,000
2,000
0
LEAK
CI
CI+CII
CII
OXPHOS

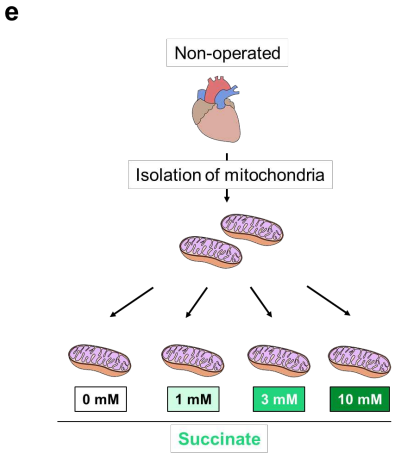
e
Non-operated
Isolation of mitochondria
0 mM
1 mM
3 mM
10 mM
Succinate

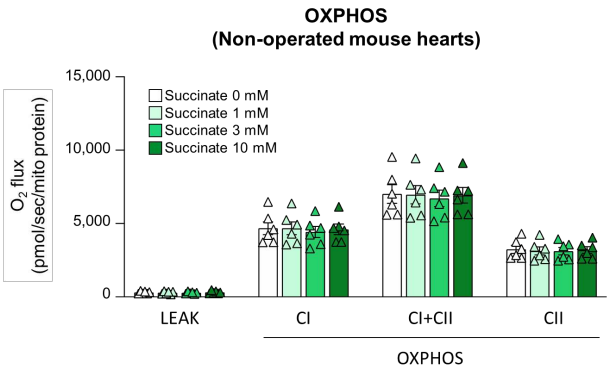
f
OXPHOS
(Non-operated mouse hearts)
Succinate 0 mM
Succinate 1 mM
Succinate 3 mM
Succinate 10 mM
O2 flux (pmol/sec/mito protein)
15,000
10,000
5,000
0
LEAK
CI
CI+CII
CII
OXPHOS

195

Fig. 3. Reduced succinyl-CoA level impairs OXPHOS activities of myocardial mitochondria during chronic HF. a, b, Experimental scheme to measure myocardial mitochondrial OXPHOS activities of MI mice and sham mice, and their responses to the addition of succinyl-CoA (**a**); and the actual results (**b**). **c**-**f**, Experimental scheme to measure myocardial mitochondrial OXPHOS activities in non-operated mice in response to the addition of succinyl-CoA (**c**) and succinate (**e**); and the actual results (**d**, **f**). In **b**, **d**, and **f**, each data point in the dot plot represents one individual mouse sample. Data are shown as the mean ± s.e.m. Data were analyzed by one-way analysis of variance (ANOVA) with the Tukey's test (**b**), or one-way ANOVA with the Dunnett's test (**d**). **P* < 0.05. LEAK, leak state

ALA prevents HF progression of MI mice (38/40 characters)

Based on our results, we next analyzed effective treatments of HF that modify mitochondrial dysfunction (*i.e.*, reduced succinyl-CoA) in MI mice. Succinyl-CoA itself is too unstable to be used as a drug, and the administration of excess succinate has been shown to be harmful to mitochondria and to promote their fragmentation and dysfunction[22]. Based on the mechanism of succinyl-CoA dysregulation in MI mice, we tested the effects of ALA. The administration of ALA to MI mice in their drinking water, which was initiated immediately after coronary artery ligation and was continued for 4 weeks, significantly improved their left ventricular (LV) function and treadmill running capacity (*i.e.*, systemic exercise capacity), and prolonged their survival (Fig. 4a-c). Likewise, the enlargement of LV-end-diastolic diameter (LVEDD), a parameter of LV remodeling, also tended to be prevented in MI mice with ALA treatment (Extended Data

Fig. 2). Molecularly, both CI- and CII-linked OXPHOS capacities of myocardial mitochondria were significantly improved in MI mice with ALA treatment (Fig. 4d). The administration of ALA also appeared to sufficiently restore succinyl-CoA levels of the myocardial mitochondria of MI mice, although a statistically significant difference was not observed between MI mice with and without ALA treatment, possibly because of the fluctuation in succinyl-CoA levels of MI mice without ALA treatment (Fig. 4e). There was no significant difference in mitochondrial heme levels between MI mice with and without ALA treatment (Fig. 4f). Taken together, the administration of ALA might be an effective treatment for the prevention of HF progression after MI. ALA functions as an intermediate of the heme synthesis from succinyl-CoA, as mentioned earlier. Our results hence also support the notion that the decrease in succinyl-CoA level in MI mice may be caused, at least in part by the excessive consumption of succinyl-CoA outside of the TCA cycle, such as in heme synthesis.

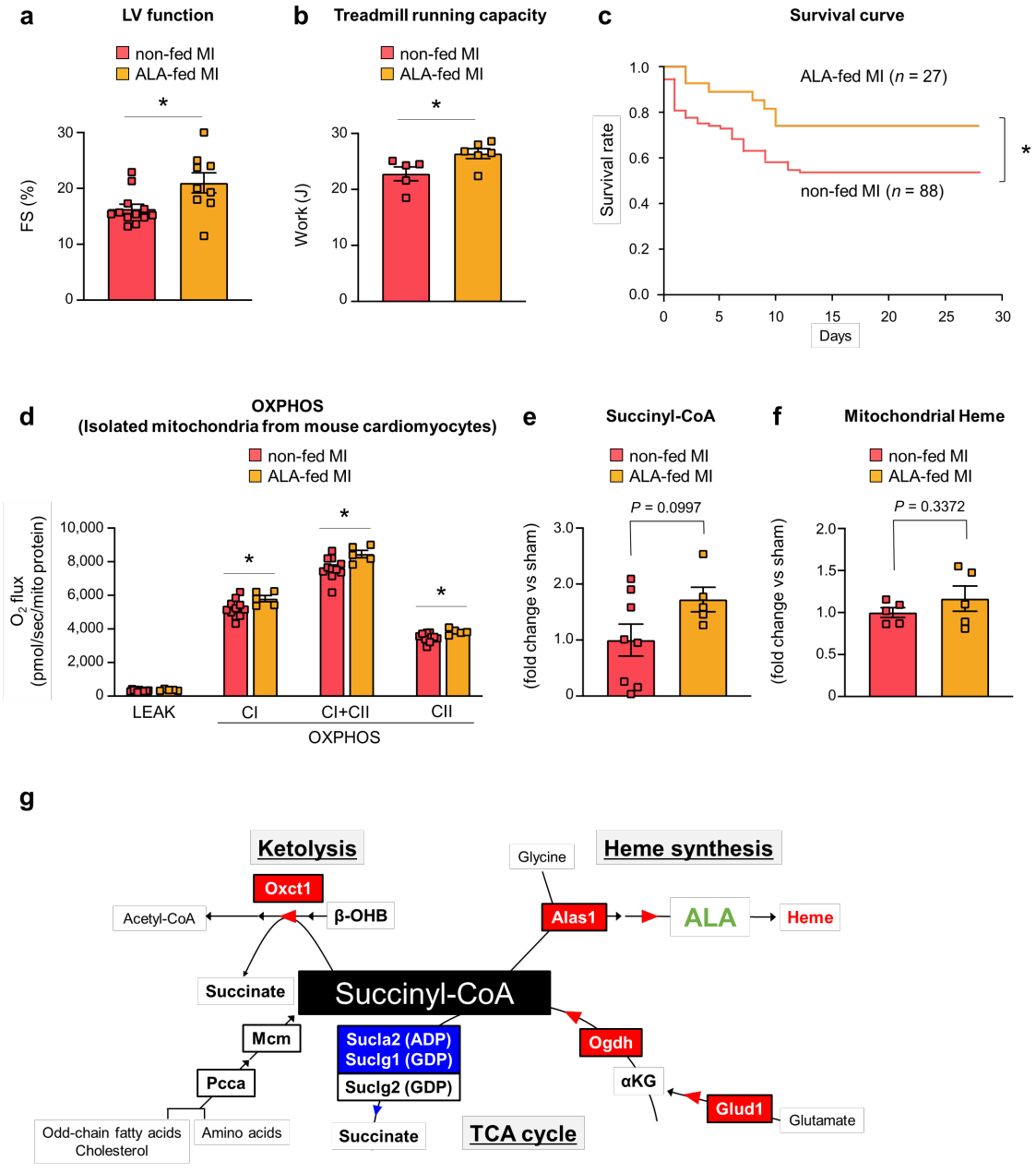

Fig. 4. Therapeutic effects of ALA against MI-induced HF. a-c, Effects of ALA on HF symptoms were analyzed by administering MI mice with or without ALA in their drinking water for 4 weeks, starting immediately after the permanent coronary artery ligation; and then measuring their LV function (*i.e.*, the percent fractional shortening (%FS)) (**a**), treadmill running capacity (**b**), and survival (**c**). **d-f**, Effects of ALA on OXPHOS activities (**d**), relative succinyl-CoA levels (**e**), and relative heme levels (**f**), measured in

myocardial mitochondria isolated from ALA-fed or non-fed MI mice. In **a**, **b**, **d-f**, data are shown as the mean ± s.e.m.. Each data point in the dot plots represents one individual mouse sample. Data were analyzed by the two-tailed Student *t*-test (**a**, **b**, **d**, **e**, **f)** and two-side log-rank test (**c**). **P* < 0.05. **g**. A proposed model of the metabolic shifts in myocardial mitochondria during chronic HF, whereby we demonstrated that ALA administration to mice can improve succinyl-CoA levels and OXPHOS activities, as well as heart function, and prolong survival.

Extended data Fig. 2

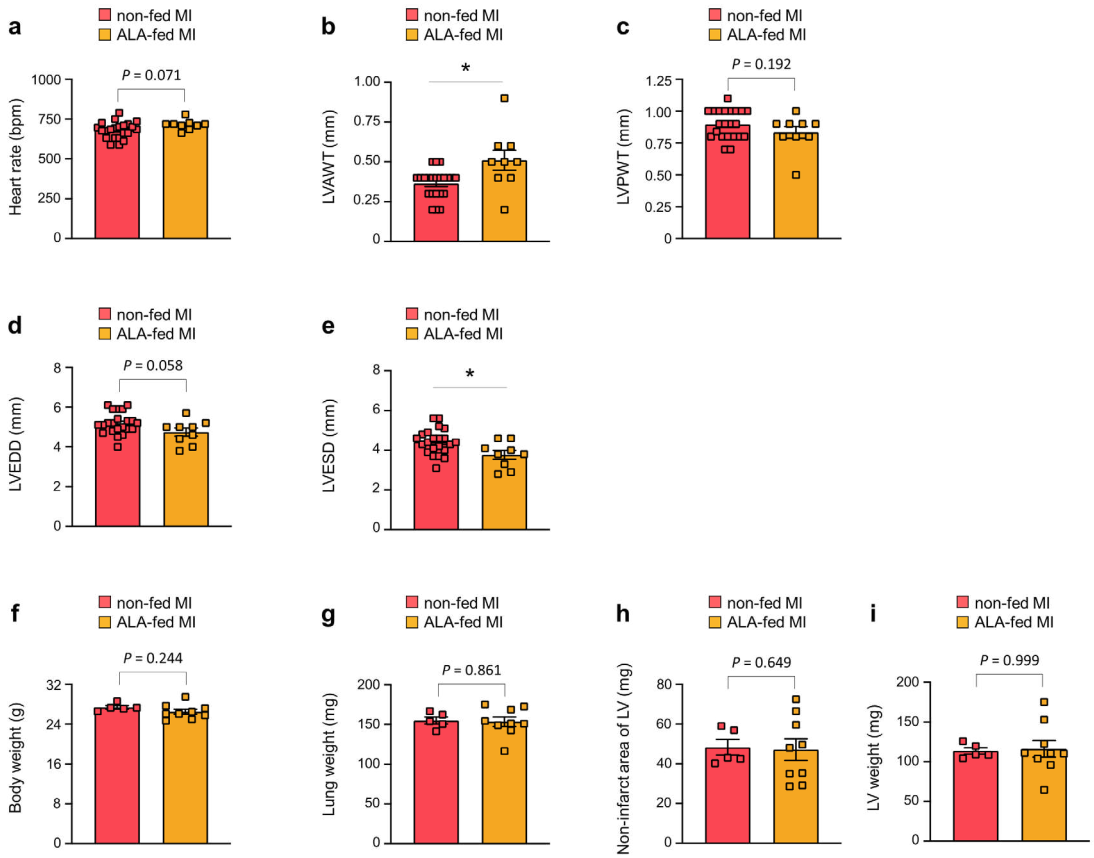

Extended Data Figure 2. Cardiac parameters of ALA-fed and non-fed MI mice. MI mice were administered with or without ALA daily in their drinking water for 4 weeks

(ALA-fed and non-fed, respectively), starting immediately after the coronary ligation, and then the following cardiac parameters were measured: heart rate (**a**), LVAWT (**b**), LVPWT (**c**), LVEDD (**d**), LVESD (**e**), body weight (**f**), lung weight (**g**), non-infarct area of LV weight (**h**), and LV weight (**i**).

Disturbed protein succinylation in HF (38/40 characters)

Succinyl-CoA is known as a source of protein succinylation[23,24]. Succinylation occurs predominantly on mitochondrial proteins in the heart, and may affect some of their enzymatic activities[25]. Decreased protein succinylation in the cardiac myofibrils of failing human hearts has been reported previously[6]. Likewise, overall levels of protein succinylation were significantly lower in the myocardial mitochondria of MI mice than in sham mice, and the incubation of isolated mitochondria from MI mice with 1 mM succinyl-CoA significantly increased protein succinylation (Extended Data Fig. 3b). In contrast, the stoichiometry of the succinylation of various proteins is unlikely to be constantly decreased in MI, as reported previously[6]. We observed that the succinylation of many TCA cycle enzymes (Extended Data Fig. 3f) and mitochondrial membrane proteins (Extended Data Fig. 3g) tended to be increased in MI mice. Sirtuin 5 (Sirt5) is the main enzyme that catalyzes Lys desuccinylation in mitochondria[26]. Levels of Sirt5 tended to be downregulated in MI mice, although we did not see a clear difference between MI mice and sham mice (Extended Data Fig. 4). Furthermore, although Sirt5 was reported to suppress SDH activity[26], we did not observe a decrease in Sdha or Sdhb succinylation in MI mice (Extended Data Fig. 3e). However, we could not rule out the possibility that some artificial events, likely caused by *in vitro* mitochondrial

manipulations, were involved in these changes. It may be noteworthy, however, that the incubation of MI mitochondria with succinyl-CoA tended to decrease the succinylation of TCA cycle enzymes and membrane proteins, which appeared to show increased succinylation in MI mice compared with sham mice (Extended Data Fig. 3f, g). On the other hand, it should also be noted that incubation with succinyl-CoA appears to cause further dysregulation of the succinylation stoichiometry of some other proteins, including Sdhb (Extended Data Fig. 3e). Collectively, our results suggest that processes regulating the succinylation/desuccinylation of myocardial mitochondrial proteins might undergo complicated, and perhaps at least partly irreversible changes in MI mice, in which the dysregulation of succinyl-CoA metabolism is likely to be among the causes. Whether the perturbed stoichiometry of mitochondrial protein succinylation affects cardiac functions requires further analyses.

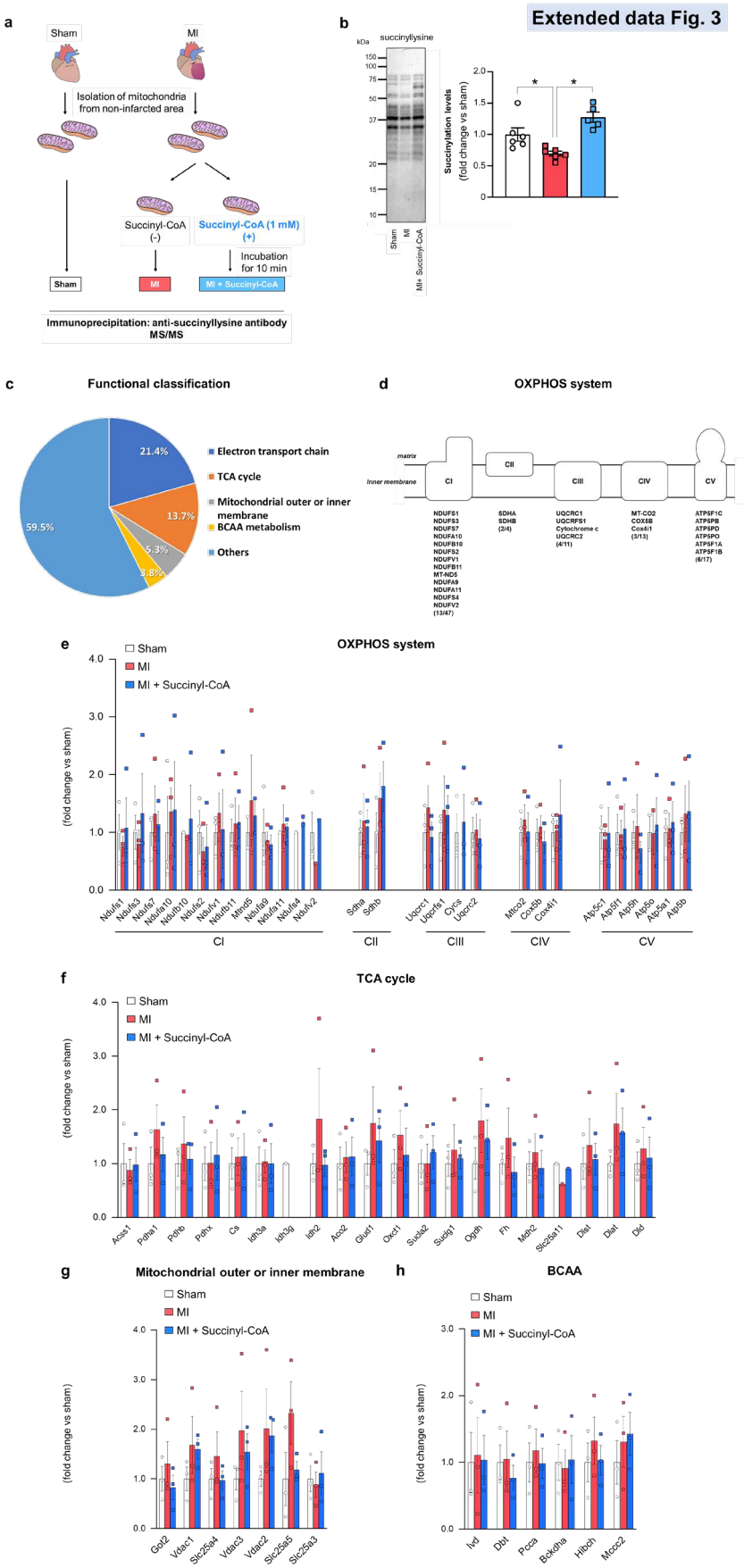
Extended data Fig. 3
a
Sham
MI
Isolation of mitochondria from non-infarcted area
Succinyl-CoA (-)
Succinyl-CoA (1 mM) (+)
Incubation for 10 min
Sham
MI
MI + Succinyl-CoA
Immunoprecipitation: anti-succinyllysine antibody MS/MS
b
succinyllysine
kDa
150
100
75
50
37
20
15
10
Sham
MI
MI+ Succinyl-CoA
Succinylation levels (fold change vs sham)
2.0
1.5
1.0
0.5
0
*
*
c
Functional classification
21.4%
13.7%
5.3%
3.8%
59.5%
Electron transport chain
TCA cycle
Mitochondrial outer or inner membrane
BCAA metabolism
Others
d
OXPHOS system
matrix
Inner membrane
CI
CII
CIII
CIV
CV
NDUFS1
NDUFS3
NDUFS7
NDUFA10
NDUFB10
NDUFS2
NDUFV1
NDUFB11
MT-ND5
NDUFA9
NDUFA11
NDUFS4
NDUFV2
(13/47)
SDHA
SDHB
(2/4)
UQCRC1
UQCRFS1
Cytochrome c
UQCRC2
(4/11)
MT-CO2
COX5B
Cox4i1
(3/13)
ATP5F1C
ATP5PB
ATP5PD
ATP5PO
ATP5F1A
ATP5F1B
(6/17)
e
OXPHOS system
Sham
MI
MI + Succinyl-CoA
(fold change vs sham)
4.0
3.0
2.0
1.0
0.0
Ndufs1
Ndufs3
Ndufs7
Ndufa10
Ndufb10
Ndufs2
Ndufv1
Ndufb11
Mtnd5
Ndufa9
Ndufa11
Ndufs4
Ndufv2
CI
Sdha
Sdhb
CII
Uqcrc1
Uqcrfs1
Cycs
Uqcrc2
CIII
Mtco2
Cox5b
Cox4i1
CIV
Atp5c1
Atp5h1
Atp5h
Atp5o
Atp5a1
Atp5b
CV
f
TCA cycle
Sham
MI
MI + Succinyl-CoA
(fold change vs sham)
4.0
3.0
2.0
1.0
0.0
Acas1
Pdha1
Pdhb
Pdhx
Cs
Idh3a
Idh3g
Idh2
Aco2
Glud1
Oxct1
Suclg2
Suclg1
Ogdh
Fh
Mdh2
Slc25a11
Dlst
Diat
Dld
g
Mitochondrial outer or inner membrane
Sham
MI
MI + Succinyl-CoA
(fold change vs sham)
4.0
3.0
2.0
1.0
0.0
Got2
Vdac1
Slc25a4
Vdac3
Vdac2
Slc25a5
Slc25a3
h
BCAA
Sham
MI
MI + Succinyl-CoA
(fold change vs sham)
3.0
2.0
1.0
0.0
Ivd
Dbt
Pcca
Bckdha
Hibch
Mccc2

288

Extended Data Figure 3. Perturbation of protein succinylation in myocardial mitochondria during chronic HF. a, b, Experimental scheme to compare protein succinylation in myocardial mitochondria isolated from MI mice with those from sham mice, and their changes in response to succinyl-CoA (**a**); and the actual results (**b**). In **b**, a representative anti-succinyllysine immunoblot of mitochondrial proteins after their separation by SDS-gel electrophoresis is shown on the left, and results of the quantification of all blots is shown on the right (n = 5 for each set of samples). **c**, Percentage of succinylated mitochondrial proteins classified based on their function. **d**, The name of each protein involved in each component of mitochondrial OXPHOS. **e**-**h**, Relative levels of succinylation of each myocardial mitochondria protein in MI mice and sham mice, and changes in the succinylation of proteins of the OXPHOS system (**e**), the TCA cycle (**f**), outer and inner membrane components (**g**), and those involved in branched-chain amino acid (BCAA) metabolism (**h**) in the myocardial mitochondria of MI mice in response to the addition of succinyl-CoA. In **b, e-h**, each data point in the dot plot represents one individual mouse sample. Data are shown as the mean ± s.e.m. In **b**, one-way ANOVA followed by the Tukey's test was performed. *$P < 0.05$

Extended data Fig. 4

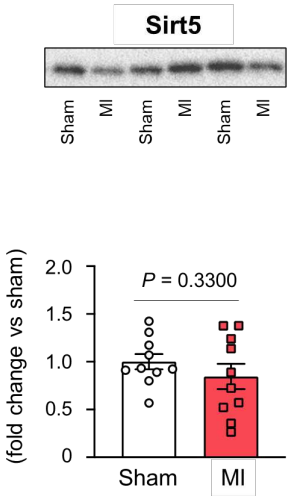

305

306 **Extended Data Figure 4. No significant changes in Sirt5 levels in myocardial**
307 **mitochondria during chronic HF.** A representative result of an immunoblot using an
308 anti-Sirt5 antibody of myocardial mitochondria proteins prepared from MI mice and sham
309 mice (upper panel); and results of the quantification of all blots (lower panel). Each data
310 point in the dot plot represents one individual mouse sample. Data are shown as the mean
311 ± s.e.m.

312

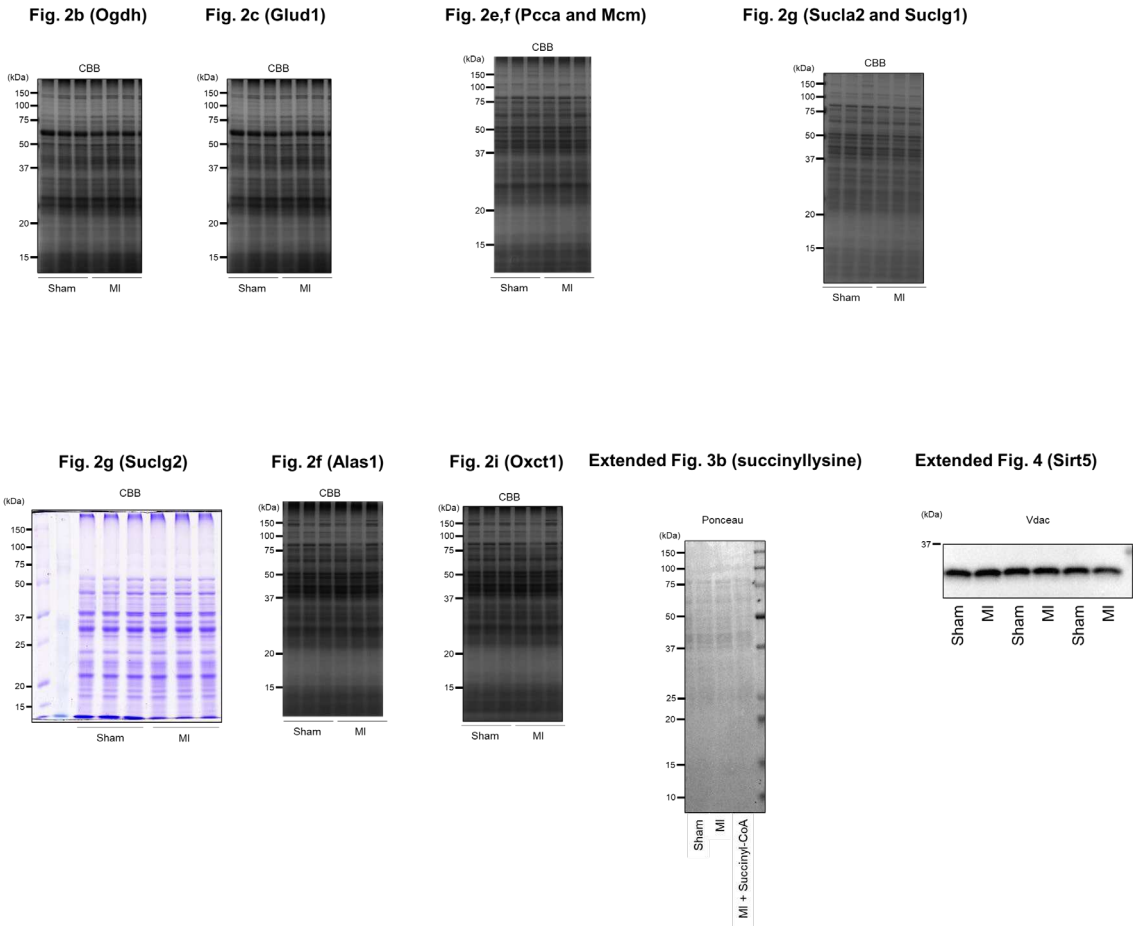

Extended Data Figure 5. Full size scans of the internal controls of the immunoblots shown in the figures of this paper.

Discussion

In this study, we identified previously unknown mechanisms underlying the metabolic dysfunction occurring in myocardial mitochondria, using a well-established mouse model of chronic HF. This dysfunction appeared to be mainly attributable to the altered expression levels of enzymes involved in mitochondrial succinyl-CoA metabolism (Fig.

4g), and a selective decrease in succinyl-CoA level was frequently observed in myocardial mitochondria during chronic HF, thus causing OXPHOS impairment. The metabolic changes that occur in chronic HF, such as ketolysis, also occur in healthy conditions, such as during strenuous exercise, although whether the same enzyme level changes also occur under healthy conditions remains unknown. Intriguingly, we also identified a selective reduction of the ADP-specific isoform of succinyl-CoA synthetase in chronic HF. Although we still do not know the molecular mechanism therein involved, RNASeq data have shown that a particular population of some HF patients demonstrate decreased expression of *SUCLG1/SUCLA2,* together with increased expression of *ALAS1* in their cardiac muscle[7,27]. The dysfunction of succinyl-CoA metabolism in cardiac myofibrils of HF patients was also suggested recently[6]. We demonstrated that nutritional intervention that compensates the altered succinyl-CoA metabolism in chronic HF is a promising method to treat this disease. Therefore, our results, as well as further understanding of the detailed metabolic changes in chronic HF, will facilitate the development of more natural treatments, as well as the prevention of the progression of HF[28]. Succinyl-CoA is the most abundant acyl-CoA in the heart[29]. Whether the mitochondrial dysfunction occurring in HF affects the histone acylations involved in epigenetic control[13] should also be clarified in the future[30].

1 Chioncel, O. *et al.* Clinical phenotypes and outcome of patients hospitalized for acute heart failure: the ESC Heart Failure Long-Term Registry. *Eur J Heart Fail* **19**, 1242-1254, doi:10.1002/ejhf.890 (2017).

2 Brown, D. A. *et al.* Expert consensus document: Mitochondrial function as a therapeutic target in heart failure. *Nat Rev Cardiol* **14**, 238-250,

347 doi:10.1038/nrcardio.2016.203 (2017).
348 3 Okonko, D. O. & Shah, A. M. Heart failure: mitochondrial dysfunction and
349 oxidative stress in CHF. *Nat Rev Cardiol* **12**, 6-8, doi:10.1038/nrcardio.2014.189
350 (2015).
351 4 Bertero, E. & Maack, C. Metabolic remodelling in heart failure. *Nat Rev Cardiol*
352 **15**, 457-470, doi:10.1038/s41569-018-0044-6 (2018).
353 5 Stojanovski, B. M. *et al.* 5-Aminolevulinate synthase catalysis: The catcher in
354 heme biosynthesis. *Mol. Genet. Metab.* **128**, 178-189,
355 doi:10.1016/j.ymgme.2019.06.003 (2019).
356 6 Ali, H. R. *et al.* Defining decreased protein succinylation of failing human
357 cardiac myofibrils in ischemic cardiomyopathy. *J. Mol. Cell. Cardiol.* **138**, 304-
358 317, doi:10.1016/j.yjmcc.2019.11.159 (2020).
359 7 Sweet, M. E. *et al.* Transcriptome analysis of human heart failure reveals
360 dysregulated cell adhesion in dilated cardiomyopathy and activated immune
361 pathways in ischemic heart failure. *BMC Genomics* **19**, 812,
362 doi:10.1186/s12864-018-5213-9 (2018).
363 8 Chouchani, E. T. *et al.* Ischaemic accumulation of succinate controls reperfusion
364 injury through mitochondrial ROS. *Nature* **515**, 431-435,
365 doi:10.1038/nature13909 (2014).
366 9 Martin, J. L. *et al.* Succinate accumulation drives ischaemia-reperfusion injury
367 during organ transplantation. *Nat Metab* **1**, 966-974, doi:10.1038/s42255-019-
368 0115-y (2019).
369 10 Zhang, J. *et al.* Accumulation of Succinate in Cardiac Ischemia Primarily Occurs
370 via Canonical Krebs Cycle Activity. *Cell Rep* **23**, 2617-2628,

doi:10.1016/j.celrep.2018.04.104 (2018).

11 Matsumoto, J. *et al.* Brain-Derived Neurotrophic Factor Improves Limited Exercise Capacity in Mice With Heart Failure. *Circulation* **138**, 2064-2066, doi:10.1161/CIRCULATIONAHA.118.035212 (2018).

12 Yu, X. *et al.* MARK4 controls ischaemic heart failure through microtubule detyrosination. *Nature* **594**, 560-565, doi:10.1038/s41586-021-03573-5 (2021).

13 Trefely, S., Lovell, C. D., Snyder, N. W. & Wellen, K. E. Compartmentalised acyl-CoA metabolism and roles in chromatin regulation. *Mol Metab* **38**, 100941, doi:10.1016/j.molmet.2020.01.005 (2020).

14 Burch, J. S. *et al.* Glutamine via alpha-ketoglutarate dehydrogenase provides succinyl-CoA for heme synthesis during erythropoiesis. *Blood* **132**, 987-998, doi:10.1182/blood-2018-01-829036 (2018).

15 Aubert, G. *et al.* The Failing Heart Relies on Ketone Bodies as a Fuel. *Circulation* **133**, 698-705, doi:10.1161/CIRCULATIONAHA.115.017355 (2016).

16 Horton, J. L. *et al.* The failing heart utilizes 3-hydroxybutyrate as a metabolic stress defense. *JCI Insight* **4**, doi:10.1172/jci.insight.124079 (2019).

17 Xie, J., Liu, X., Li, Y., Liu, Y. & Su, G. Validation of RT-qPCR reference genes and determination of Robo4 expression levels in human retinal endothelial cells under hypoxia and/or hyperglycemia. *Gene* **585**, 135-142, doi:10.1016/j.gene.2016.03.047 (2016).

18 Khechaduri, A., Bayeva, M., Chang, H. C. & Ardehali, H. Heme levels are increased in human failing hearts. *J. Am. Coll. Cardiol.* **61**, 1884-1893, doi:10.1016/j.jacc.2013.02.012 (2013).

19 Evans, M., Cogan, K. E. & Egan, B. Metabolism of ketone bodies during exercise and training: physiological basis for exogenous supplementation. *J Physiol* **595**, 2857-2871, doi:10.1113/JP273185 (2017).

20 Maekawa, S. *et al.* Linoleic acid improves assembly of the CII subunit and CIII2/CIV complex of the mitochondrial oxidative phosphorylation system in heart failure. *Cell Commun Signal* **17**, 128, doi:10.1186/s12964-019-0445-0 (2019).

21 Martinez-Reyes, I. & Chandel, N. S. Mitochondrial TCA cycle metabolites control physiology and disease. *Nat Commun* **11**, 102, doi:10.1038/s41467-019-13668-3 (2020).

22 Pfleger, J., He, M. & Abdellatif, M. Mitochondrial complex II is a source of the reserve respiratory capacity that is regulated by metabolic sensors and promotes cell survival. *Cell Death Dis* **6**, e1835, doi:10.1038/cddis.2015.202 (2015).

23 Wagner, G. R. & Payne, R. M. Widespread and enzyme-independent Nepsilon-acetylation and Nepsilon-succinylation of proteins in the chemical conditions of the mitochondrial matrix. *J. Biol. Chem.* **288**, 29036-29045, doi:10.1074/jbc.M113.486753 (2013).

24 Yang, Y. & Gibson, G. E. Succinylation Links Metabolism to Protein Functions. *Neurochem. Res.* **44**, 2346-2359, doi:10.1007/s11064-019-02780-x (2019).

25 Wagner, G. R. *et al.* A Class of Reactive Acyl-CoA Species Reveals the Non-enzymatic Origins of Protein Acylation. *Cell Metab* **25**, 823-837 e828, doi:10.1016/j.cmet.2017.03.006 (2017).

26 Park, J. *et al.* SIRT5-mediated lysine desuccinylation impacts diverse metabolic pathways. *Mol. Cell* **50**, 919-930, doi:10.1016/j.molcel.2013.06.001 (2013).

27 Ramirez Flores, R. O. *et al.* Consensus Transcriptional Landscape of Human End-Stage Heart Failure. *J Am Heart Assoc* **10**, e019667, doi:10.1161/JAHA.120.019667 (2021).

28 Takada, S., Sabe, H. & Kinugawa, S. Abnormalities of Skeletal Muscle, Adipocyte Tissue, and Lipid Metabolism in Heart Failure: Practical Therapeutic Targets. *Front Cardiovasc Med* **7**, 79, doi:10.3389/fcvm.2020.00079 (2020).

29 Sadhukhan, S. *et al.* Metabolomics-assisted proteomics identifies succinylation and SIRT5 as important regulators of cardiac function. *Proc. Natl. Acad. Sci. U. S. A.* **113**, 4320-4325, doi:10.1073/pnas.1519858113 (2016).

30 Gilsbach, R. *et al.* Distinct epigenetic programs regulate cardiac myocyte development and disease in the human heart in vivo. *Nat Commun* **9**, 391, doi:10.1038/s41467-017-02762-z (2018).

Methods

Animal procedures and ethics statement

Animal experiments were performed according to a protocol approved by the Animal Care Committee of Hokkaido University (study approval no.: 16-0115). C57BL/6J mice were used in all experiments, and were housed under standard conditions (temperature: 23–25 °C, and humidity: 40%–60%) on a 12-h light/dark cycle.

In vivo HF mouse model

As an *in vivo* HF model, a coronary ligated model was used, as described previously[11]. Permanent left anterior descending (LAD) coronary artery ligation was performed on the mice. Male C57BL/6J mice (9–12 weeks old; CLEA Japan) were anesthetized with an intraperitoneal injection of a mixture of 0.3 mg/kg body weight of medetomidine (Kyoritsu, Dorbene®), 4.0 mg/kg body weight of midazolam (Astellas, Dormicum®), and 5.0 mg/kg body weight of butorphanol (Meiji, Vetorphale®) (MMB mixture), and then intubated and ventilated with air (supplemented with oxygen) using a small-animal respirator. The adequacy of anesthesia was monitored by the pedal withdrawal reflex. A thoracotomy was performed in the fourth left intercostal space. Then, the left ventricle was visualized and the pericardial sac was ruptured to expose the LAD coronary artery. The LAD was permanently ligated using a 4-0 Prolene suture (Covidien, Sofsilk™ VS-709). The suture was passed approximately 0.5 mm below the tip of the left auricle. Sham-operated mice, which were used as controls, underwent thoracotomy of the heart as in coronary-ligated mice, except that their arteries were not tied. The thoracotomy was closed with 8-0 Prolene sutures (Akiyama Medical MFG, M6-80B2). The endotracheal tube was removed once spontaneous respiration resumed, and the mice were placed in a

warm recovery cage maintained at 37 °C until they were completely awake. After 4 weeks, mice were subjected to analyses. For biochemical analysis, mice were sacrificed with an intraperitoneal injection of the MMB mixture, and the heart was then excised and subjected to analyses. Regarding the LVs of HF mice, the infarct areas were excluded from the biochemical analyses, and only noninfarct areas were used for the experiments. Blood samples of the mice were collected from the inferior vena cava before euthanization by deep anesthesia with the MMB mixture, as described previously[31].

Metabolite extraction from mouse heart

Mice were sacrificed by cervical dislocation under general anesthesia. Mouse LVs, excluding the infarcted areas, were isolated within 2 min after cervical dislocation, and rapidly cryopreserved with liquid nitrogen. Pieces of the mouse LV (40–50 mg) were snap-frozen in liquid nitrogen and crushed using a MultiBeads Shocker (Bio Medical Science) at 2,000 rpm for 10 sec. The crushed powder was then dissolved in 1 mL of ice-cold 80% methanol per 100 mg tissue weight, sonicated five times (five rounds of sonication for 30 secs and cooling for 30 secs) using a BIORUPTOR (Cosmo Bio), and centrifuged at 21,500 *g* for 5 min at 4 °C. The supernatants were then collected and subjected to LC-MS analyses.

Metabolite analysis by LC-MS

To measure the TCA cycle intermediates, heart lysate supernatants (equivalent to approximately 1.5 mg of the heart) were applied and separated on an ACQUITY BEH C18 column (100 mm × 2.1 mm, 1.7 μm, Waters™, 186002352) and analyzed using an LCMS 8040 instrument (Shimadzu) by multiple reaction monitoring of 98 specific

479 negative ions, as described previously[32]. The mobile phase consisted of 15 mM acetic
480 acid and 10 mM tributylamine in 3% methanol solution (A) and 100% methanol (B). The
481 gradient elution program was as follows: 0–6 min, 0% B; 6–26 min, 0%–90% B;
482 decreased to 0% B and maintained until 15 min. The flow rate was 0.3 mL/min, and the
483 column oven temperature was 40 °C. Parameters for the negative electrospray ionization
484 mode were as follows: drying gas flow rate, 15 L/min; nebulizer gas flow rate, 3 L/min;
485 heating gas flow rate, 10 L/min; desolvation line temperature, 250 °C; and heat block
486 temperature, 400 °C; collision induced dissociation gas, 230 kPa. Data processing was
487 performed using LabSolutions software (Shimadzu) and signal intensities were
488 standardized against the signals of MES.
489
490 **Isolation of mitochondria from mouse heart**
491 Mitochondria were isolated as described previously[20]. Briefly, excised mouse hearts were
492 quickly minced using scissors for 4 min, and incubated with 0.1 mg/mL proteinase
493 (Sigma-Aldrich, P8038) for 2 min at 4 °C in mitochondrial isolation buffer containing 50
494 mM Tris-HCl (pH 7.4), 100 mM KCl, 100 mM sucrose, 1 mM KH_2PO_4, 0.1 mM EGTA,
495 and 0.2% bovine serum albumin. They were then gently homogenized using a motor-
496 driven Teflon pestle in a glass chamber (Wheaton, 358039) with six strokes, and
497 centrifuged at 700 *g* for 10 min. Supernatants were recentrifuged at 10,000 *g* for 10 min,
498 and pellets were then suspended in the mitochondrial isolation buffer, after washing
499 briefly once with the same buffer, and centrifuged again at 7,000 *g* for 3 min. The resulting
500 pellets were resuspended in a buffer containing 10 mM Tris-HCl (pH 7.4), 225 mM
501 mannitol, 75 mM sucrose, and 0.1 mM EDTA, and subjected to analyses. All procedures,
502 except for the preincubation with proteinase, were performed at 4 °C. Protein

503 concentrations of the samples were measured using the bicinchoninic acid assay (Thermo
504 Fisher Scientific, 23225).
505
506 **Immunoblotting analysis**
507 Immunoblotting analysis was performed as described previously[33]. Briefly, mitochondrial
508 proteins were denatured in Laemmli buffer (100 mM Tris-HCl [pH 6.8], 4% SDS, 4%
509 glycerol, 0.05% bromophenol blue, 12% 2-mercaptoethanol) at 100 °C for 5 min,
510 separated by SDS-PAGE using Any kD™ Criterion™ precast gels (Bio-Rad,
511 5671122J10), and transferred to polyvinylidene fluoride membranes (Bio-Rad, cat. no.:
512 1704156). Membranes were then blocked for 1 h at room temperature in TBS-T buffer
513 (0.1%Tween-20 in 1 × PBS) containing 3% milk, and incubated with primary antibodies
514 diluted in TBS-T with 3% milk, overnight at 4 °C. Primary antibodies used were as
515 follows: Sucla2 (Abcam, ab202582, 1:1,000 dilution), Suclg1 (Abcam, ab204432,
516 1:1,000 dilution), Suclg2 (Abcam, ab241375, 1:1,000 dilution), Glud1 (Abcam, ab
517 168352, 1:1,000 dilution), Ogdh (Abcam, ab137773, 1:1,000 dilution), Alas1 (Abcam,
518 ab84962, 1:1,000 dilution), Oxct-1 (Abcam, ab105320, 1:1,000 dilution), Pcca (Abcam,
519 ab187686, 1:1,000 dilution), Mcm (Abcam, ab134956, 1:1,000 dilution), Sirt5 (Abcam,
520 ab13697, 1:1,000 dilution) and succinyllysine (PTM BIO, PTM419, 1:1,000 dilution).
521 After three washes with TBS-T, membranes were then incubated with a horseradish
522 peroxide-conjugated secondary antibody (Abcam, ab97051, 1:20,000 dilution, or Santa
523 Cruz, sc-2314, 1:5,000 dilution) in TBS-T with 3% milk, for 1 h at room temperature.
524 After washing, peroxide-conjugated Abs retained on membranes were visualized with the
525 enhanced chemiluminescence kit (Thermo Fisher Scientific, 32106 or 34075) coupled
526 with ChemiDoc XRS$^+$ (Bio-Rad). Densities of the signals were quantified with Image J

software (U.S. National Institutes of Health). Expression levels of the proteins are shown as values normalized by the protein level of voltage-dependent anion channel, which is a representative mitochondrial marker (Cell Signaling Technology, 4866, 1:1,000 dilution), or total amounts of proteins measured by Coomassie brilliant blue (CBB) staining (Bio-Rad, 1610786) or Ponceau-S staining (Beacle, BCL-PSS-01).

Measurement of mitochondrial OXPHOS activities

To assess mitochondrial OXPHOS, respiration capacities of isolated mitochondria were measured with a high-resolution respirometer (Oxygraph-2k, Oroboros)[11]. Isolated mitochondria (approximately 30–100 μg) were placed into the respirometer chamber, filled with 2 mL of MiR05 medium (110 mmol/L sucrose, 60 mmol/L K-lactobionate, 0.5 mmol/L EGTA, 0.1% BSA, 3 mmol/L $MgCl_2$, 20 mmol/L taurine, 10 mmol/L KH_2PO_4, 20 mmol/L HEPES, pH 7.1), and then incubated with chemicals at 37 °C in the following order (final concentrations are indicated): (1) 2 mM malate, 5 mM pyruvate, 10 mM glutamate (complex I-linked substrates), (2) 10 mM ADP, and (3) 10 mM succinate (complex II-linked substrate) and 0.5 μM rotenone (a complex I inhibitor). The O_2 consumption rates (*i.e.*, respiration rates) were expressed as O_2 flux normalized to the mitochondrial protein concentration (μg/μL). DatLab software (Oroboros) was used for data acquisition and analysis.

Measurement of mitochondrial heme

Intra-mitochondrial heme was quantified using the QuantiChrom™ Heme Assay Kit (BioaAssay Systems, DIHM-250), according to the manufacture's instruction. Briefly, isolated mitochondria were mixed with 200 μL of reaction mixture provided with the

assay kit, and incubated for 5 min at room temperature. Optical densities at 400 nm were then measured in a microtiter plate reader (Multiskan GO, Thermo Fisher), in which the standard curve was prepared using a heme standard provided by the assay kit.

Measurement of plasma and heart beta-hydroxybutyrate

β-OHB levels in the plasma and hearts were measured using the β-OHB Assay Kit (Abcam, ab180876), according to the manufacture's instruction.

Feeding mice with ALA

Mice were divided into two groups after coronary ligation; one group was given normal-water, and the other was given water containing 50 mg/L ALA (Sigma Aldrich, A3785), and the amount of ALA ingested was 6 to 8 mg/kg body weight per day. After 4 weeks, mice were subjected to echocardiography and treadmill running, and then sacrificed with an intraperitoneal injection of the MMB mixture, for subsequent biochemical analyses.

Echocardiography

Echocardiographic measurements were performed in mice in the conscious state to avoid any effects of anesthesia on cardiac function, as described previously[33]. Briefly, a commercially available echocardiography system (Toshiba Medical Systems, Aplio^{TM}300) was used with a dynamically focused 12-MHz linear array transducer and a depth setting of 2.0 cm. The fur on the chest was removed using depilatory cream and a layer of acoustic coupling gel was applied to the thorax. A two-dimensional parasternal short-axis view was obtained at the levels of the papillary muscles. In general, the clearest views were obtained with the transducer lightly applied to the mid-upper left anterior

chest wall. The transducer was then gently moved in the cephalad or caudad direction, and angulated until desirable images were obtained. After confirmation that the imaging was on the axis, two-dimensional targeted M-mode tracings were recorded at a paper speed of 50 mm/sec. The following indexes were analyzed using the software in the echo instrument: LVEDD, LV end-systolic diameter (LVESD), percent fractional shortening (%FS), heart rate (HR), anterior wall thickness (AWT), and posterior wall thickness (PWT) of the LV.

Treadmill running

Mice were subjected to treadmill running to assess their whole-body exercise capacity, as previously described[31]. Briefly, each mouse was made to run on a motor-driven treadmill enclosed within a chamber with constant air flow, in which the O_2 and CO_2 fractions were monitored (Oxymax 2; Columbus Instruments). After a 10-min warm-up at 6 m/min at 0° inclination, the treadmill angle was fixed at 10° and the speed was gradually increased by 2 m/min until the mouse attained exhaustion. Exhaustion was defined as spending more than 10 sec on the electrical shocker plate without attempting to go back onto the treadmill. Work as whole-body exercise capacity was defined as the product of the vertical running distance to exhaustion, and body weight.

Protein succinylation of mitochondria

Mitochondria isolated from mouse cardiac muscles were denatured in buffer (1% SDS and 0.07% 2-mercaptoethanol in PBS) and boiled for 10 min. Mitochondrial proteins were then incubated with an anti-succinyllysine antibody conjugated with agarose beads (PTM Biolabs, PTM419) at 4 °C with gentle rotation overnight. After washing three times

599 with buffer (0.05% Lauryl Maltoside in PBS), the beads were dissolved in Laemmli buffer
600 and boiled for 5 min. Supernatants were then collected after brief centrifugation, and
601 subjected to MS/MS. After reduction with 10 mM TCEP (FUJIFILM Wako Chemicals,
602 203-20153) at 100 °C for 10 min and alkylation with 50 mM iodoacetamide (FUJIFILM
603 Wako Chemicals, 093-02152) at ambient temperature for 45 min, protein samples were
604 subjected to SDS-PAGE. Electrophoresis was stopped at the migration distance of 2 mm
605 from the top edge of the separation gel. After CBB-staining, protein bands were excised,
606 destained, and cut finely prior to in-gel digestion with Trypsin/Lys-C Mix (Promega,
607 V5072) at 37 °C for 12 h. The resulting peptides were extracted from gel fragments and
608 analyzed with Orbitrap Fusion Lumos mass spectrometer (Thermo Scientific) combined
609 with UltiMate 3000 RSLC nano-flow HPLC (Thermo Scientific). Peptides were enriched
610 using μ-Precolumn (0.3 mm i.d. × 5 mm, 5 μm, Thermo Scientific, 160454) and separated
611 on an AURORA column (0.075 mm i.d. × 250 mm, 1.6 μm, Ion Opticks Pty,
612 AUR25075C18AC) using the following two-step gradient: 2% to 40% acetonitrile for
613 110 min, followed by 40% to 95% acetonitrile for 5 min in the presence of 0.1% formic
614 acid. The analytical parameters of Orbitrap Fusion Lumos were set as follows: resolution
615 of full scans = 50,000, scan range (m/z) = 350–1,500, maximum injection time of full
616 scans = 50 msec, AGC target of full scans = 4×10^5, dynamic exclusion duration = 30
617 sec, cycle time of data dependent MS/MS acquisition = 2 sec, activation type = HCD,
618 detector of MS/MS = ion trap, maximum injection time of MS/MS = 35 msec, AGC target
619 of MS/MS = 1×10^4.

620 The MS/MS spectra were searched against the *Mus musculus* protein sequence
621 database in SwissProt using Proteome Discoverer 2.4 software (Thermo Scientific), in
622 which peptide identification filters were set at “false discovery rate < 1%”. Label-free

relative quantification analysis of proteins was performed with the default parameters of Minora Feature Detector node, Feature Mapper node, and Precursor Ions Quantifier node in Proteome Discoverer 2.4 software.

Statistics and reproducibility

Data are expressed as the mean ± the s.e.m. Statistical analyses were performed using the Student *t*-test for comparisons between two groups, and by ANOVA followed by the Tukey test for comparisons between three groups using GraphPad Prism 6 software (GraphPad, San Diego, CA). The Dunnett's method was used for multiple comparisons with a control group. A univariate linear regression model was used to determine the correlations between two variables. For all animal experiments, all stated replicates are biological replicates. A *p*-value of less than 0.05 was considered to indicate a statistically significant difference between groups. Kaplan-Meier analysis with the log-rank test was performed to compare survival rates among 2 groups for 28 days MI-postsurgery. For ALA treatment studies, mice were randomly assigned to treatment groups. For mass spectrometry analyses, samples were processed in random order and experimenters were blinded to the experimental conditions. All experiments were successfully repeated with similar results at least two or three times.

Data reporting

No statistical methods were used to predetermine sample size. For *in vivo* experiments in which grouping was based on surgery, mice in the MI group were randomly chosen for the experiments. For *in vivo* experiments in which grouping was based on ALA treatment, mice in the MI group were randomly allocated to treatment groups. The investigators

were not blinded to allocation during the experiments and outcome assessment. Further information on randomization and blinding is available in the Nature Research Reporting Summary linked to this article.

Reporting summary

Further information on the research design is available in the Nature Research Reporting Summary linked to this article.

Data availability

All of the associated raw data presented in this paper are available from the corresponding author upon request. Source data are provided with this paper. Full scans for all western blots are provided in Supplementary Information. All other data are available from the corresponding author on reasonable request. Source data are provided with this paper.

31 Nambu, H. *et al.* Inhibition of xanthine oxidase in the acute phase of myocardial infarction prevents skeletal muscle abnormalities and exercise intolerance. *Cardiovasc. Res.* **117**, 805-819, doi:10.1093/cvr/cvaa127 (2021).

32 Saito, T. *et al.* Cardiomyocyte-specific loss of mitochondrial p32/C1qbp causes cardiomyopathy and activates stress responses. *Cardiovasc. Res.* **113**, 1173-1185, doi:10.1093/cvr/cvx095 (2017).

33 Furihata, T. *et al.* Cardiac-specific loss of mitoNEET expression is linked with age-related heart failure. *Commun Biol* **4**, 138, doi:10.1038/s42003-021-01675-4 (2021).

Acknowledgments The authors thank Yuki Kimura and Miwako Yamane for their technical assistance, Ayae Oda, Misaki Kihara, Naoko Toshiro, Tsukusu Yamanaka, and Misato Kobayashi for secretarial support, and H.A. Popiel for her critical reading of the manuscript. This work was supported in part by Japanese Grants-In-Aid for Scientific Research (JP17H04758 [S.T.], 18H03187 [S.K.]), Grant-In-Aid for Challenging Exploratory Research (19K22791 to S.T.), grants from the Japan Foundation for Applied Enzymology (S.T.), the MSD Life Science Foundation (S.T.), the Uehara Memorial Foundation (S.T.), the Cardiovascular Research Fund of Tokyo (S.T.), the Fukuda Memorial Foundation for Medical Research (S.T.), the SENSHIN Medical Research Foundation (S.T.), and JST COI Grant Number JPMJCE1301.

Author contributions S.T., S.M., S.K., and H.S. conceived the project. S.T., S.M., S.K., and H.S. designed the experiments. S.T., S.M., T.F., N.K., D.S., K.U., H.N., H.Hagiwara., H.Handa., Y.F., S.H., A.F., T.Y., and D.K. collected, assembled, analyzed, and interpreted the data. S.T., S.M., S.K., and H.S. wrote the paper. S.T., S.K., and H.S. critically revised the manuscript. All authors approved the final version of the manuscript and agree to be accountable for all aspects of the work.

Competing interests The authors declare no competing interests associated with this study.

Supplementary Files

This is a list of supplementary files associated with this preprint. Click to download.

- ExtendedDataFiguresSucCoA.pdf
- SupplementaryinformationsuccinylCoA.pdf